Landau theory of the size-driven phase transition in ferroelectrics

1995 J. Phys.: Condens. Matter 7 7163

(http://iopscience.iop.org/0953-8984/7/36/006)

J. Phys.: Condens. Matter 7 (1995) 7163–7171. Printed in the UK

Landau theory of the size-driven phase transition in ferroelectrics

C L Wang†‡ and S R P Smith†

† Department of Physics, University of Essex, Wivenhoe Park, Colchester CO4 3SQ, UK
‡ Department of Physics, Shandong University, Jinan, 250100, People's Republic of China

Received 22 May 1995, in final form 3 July 1995

Abstract. The influence of size on the dielectric behaviour of ferroelectrics is discussed using phenomenological Landau theory. Three types of free-standing geometry are used in our calculations—film, cylinder and sphere. For films, there is a size-driven phase transition (i.e. a transition from a ferroelectric state to a paraelectric state as the thickness of the film is decreased) so long as the surface ferroelectricity is weaker than that of bulk. The polarization becomes zero below a critical size at which the susceptibility has a maximum. Otherwise the susceptibility decreases as the film thickness decreases and no size-driven phase transition exists. However, for cylinders and spheres there is always a size-driven phase transition, and so the dielectric susceptibility is always enhanced at small size. The sphere geometry has the largest critical size amongst the three geometries. In order to fit the experimental measurements on fine-grained samples, we renormalize our calculations for the sphere geometry using a Gaussian distribution function to represent the variation of particle size. The renormalization rounds the peak in the susceptibility and noticeably shifts its position to smaller size if the standard deviation of the size distribution is comparable with its mean. The critical size judged from dielectric measurements could therefore be smaller than that of an isolated sphere. Our calculations are in qualitative agreement with experimental measurements on the susceptibility of barium titanate and lead titanate.

1. Introduction

Many measurements have shown that the dielectric constant of ferroelectrics is amplified at small size. It has been reported that the dielectric constant of fine-grained barium titanate ceramics [1] has a maximum at about 0.8–1 μm, and strongly decreases when the grain size is smaller than 0.7 μm. Similar measurements show that barium titanate made using metallo-organic decomposition technology [2] has a maximum at a grain size of around 0.4 μm. In crystallized amorphous lead titanate, the dielectric function has a maximum at an average grain size of about 100 nm [3]. All of these are indicative of a size-driven phase transition. The size at which the susceptibility is maximum is expected to coincide with the critical size (at which the polarization disappears), but this relationship has not been properly established since few experimental measurements of both susceptibility and polarization have been performed.

However, the critical size itself is still very controversial. From a study of the dependence of crystal structure on particle size, Uchino *et al* [4] reported that the critical size is about 100 nm to 200 nm in barium titanate. The ferroelectricity disappears in a barium titanate/polymer composite at around the same size range [5]. From x-ray diffraction and second-harmonic generation measurement, Schlag and Eicke [6] obtained the value 49 nm

0953-8984/95/367163+09$19.50

for the critical size of barium titanate. Stable suspensions of barium titanate particles with average radius about 10 nm are still ferroelectric [7]. However, no polarization reversal hysteresis was detected in a film with average grain size of 25 nm [8]. Films obtained from metallo-organic decomposition processing with average grain size 34 nm were not ferroelectric [9]. For lead titanate, the critical size determined from soft mode measurements by Raman scattering is 12.6 nm [10], and that measured by specific heat is 8.8 nm [11]. More recent x-ray diffraction measurements showed that lead titanate is still ferroelectric at a size of 15 nm [12]. All these results give much smaller values for the critical size than those obtained from dielectric constant measurement.

Moreover Cho *et al* [13] reported that the dielectric constant has an anomaly at around the Curie temperature in a barium titanate film with thickness of about 90 nm. As the film is fine-grained, the critical size is expected to be smaller than 90 nm. This size is much smaller than that from the earlier dielectric measurement, but lies in the region found in [6] and [4]. Another dielectric measurement report by Nagatoma [14] showed that the dielectric constant decreases with film thickness. However, the film is fine-grained with an average size between 40 nm and 70 nm. No measurement on the polarization was reported.

Landau theory has long been successfully used to explain the phase transition properties of the bulk ferroelectrics [15]. In the past few years, it has also been extended to study the surface and size effect on ferroelectrics with film or sphere structure. The film thickness dependences of the Curie temperature [16], spontaneous polarization [17, 18] and susceptibility [19, 20] have been obtained. For films, the ferroelectricity is enhanced if the surface ferroelectricity is stronger. It is reduced when the surface ferroelectricity is weaker and then there is a size-driven phase transition. However, for particles [21, 22] and cylinders [23], Landau theory predicts that the ferroelectricity is always suppressed at small size and a size-driven phase transition always exists. Experimental evidence in support of this assertion is not yet altogether convincing.

In this paper, we try to throw some light on the dielectric behaviour of ferroelectrics at small size. In section 2 we present the basic expressions for the Landau free energy, and details of the calculations of polarization and susceptibility for isolated films, cylinders and spheres are given in section 3. A comparison of the calculations with experimental measurements is given in section 4; in the case of ceramic samples, the calculations are renormalized assuming a Gaussian distribution of spherical particle size. The results are summarized in section 5.

2. Landau free energy

For a finite system, the total free energy is used instead of the free energy density normally used for an infinite and homogeneous system [24, 25]. The free energy difference between the ferroelectric and paraelectric phases has the form [26]

$$F = \int_v \mathrm{d}v \left[\frac{1}{2}AP^2 + \frac{1}{4}BP^4 + \frac{1}{6}CP^6 + \frac{1}{2}D(\nabla P)^2 - E_{ext}P\right] + \frac{D}{2\delta}\int_S P^2 \,\mathrm{d}S \tag{1}$$

where P is the polarization, $A = A_0(T - T_0)$, T is the absolute temperature, T_0 is the Curie–Weiss temperature, and A_0 as well as B, C, D and δ are material parameters. The first three terms in the first integral are the conventional free energy densities describing an infinite and homogeneous system. The gradient term measures the distortion energy from the polarization inhomogeneity. E_{ext} is an external electric field in the conventional sense. The second integral is performed on the surface of the system. It is from this term that the

surface effect comes, and the so-called extrapolation length δ measures the strength of the surface effect.

The Euler–Lagrange equation is obtained by minimizing the free energy (1)

$$D\,\nabla^2 P = AP + BP^3 + CP^5 - E_{ext} \tag{2}$$

and (1) also leads to the boundary condition

$$\frac{\partial P}{\partial n} + \frac{P}{\delta} = 0 \tag{3}$$

where n is the unit length along the normal direction of the surface. The susceptibility is defined as

$$\chi = \frac{1}{\epsilon_0}\frac{\partial P}{\partial E_{ext}} \tag{4}$$

at $E_{ext} = 0$. So we have the differential equation for susceptibility as

$$D\,\nabla^2\chi = (A + 3BP^2 + 5CP^4)\chi - 1/\epsilon_0 \tag{5}$$

and its corresponding boundary condition is

$$\frac{\partial \chi}{\partial n} + \frac{\chi}{\delta} = 0 \tag{6}$$

where the polarization P in equation (5) is the spontaneous polarization, which can be obtained from equations (2) and (3) in the absence of the external electrical field.

Generally, the extrapolation length δ depends on the inter-site interaction as well as the coordinate number within the surface layer. For a film this length is independent of film thickness, because the surface coordination number does not change with the film thickness. However, for cylinder and sphere structures, the coordination number decreases as size decreases, so the extrapolation length changes with size. We denote the extrapolation length at infinite size as δ_f, where the subscript f means film. By comparing with a microscopic model [26], the extrapolation length of a sphere δ_s can be expressed as [21, 22]

$$\frac{1}{\delta_s} = \frac{5}{d} + \frac{1}{\delta_f}\left(1 - \frac{a_0}{d}\right) \tag{7}$$

where a_0 is the lattice constant and d is the diameter. As $d \gg a_0$ in most cases, the above expression can be simplified to

$$\frac{1}{\delta_s} = \frac{5}{d} + \frac{1}{\delta_f}. \tag{8}$$

Similarly the extrapolation length for a cylinder is

$$\frac{1}{\delta_c} = \frac{5}{2d} + \frac{1}{\delta_f}. \tag{9}$$

Equation (8) and (9) are used in our calculations.

3. Calculations and results

The geometries used in the calculation are shown in figure 1. For the film geometry, we use Cartesian coordinates: the z-axis is normal to the surface, and the polarization $P(z)$ is a function of z only. For the cylinder geometry, cylindrical coordinates are used; we assume that the direction of the polarization is along the length of the cylinder (z-axis) and that its magnitude $P(r)$ depends only upon the radial position r. Spherical coordinates are used in the sphere geometry, and the problem here is simplified by the assumptions that the

polarization is along the z-axis, as shown in the figure, and that its magnitude $P(r)$ again depends only upon the radial coordinate r. Even with this simplification the numerical calculation is still very tedious.

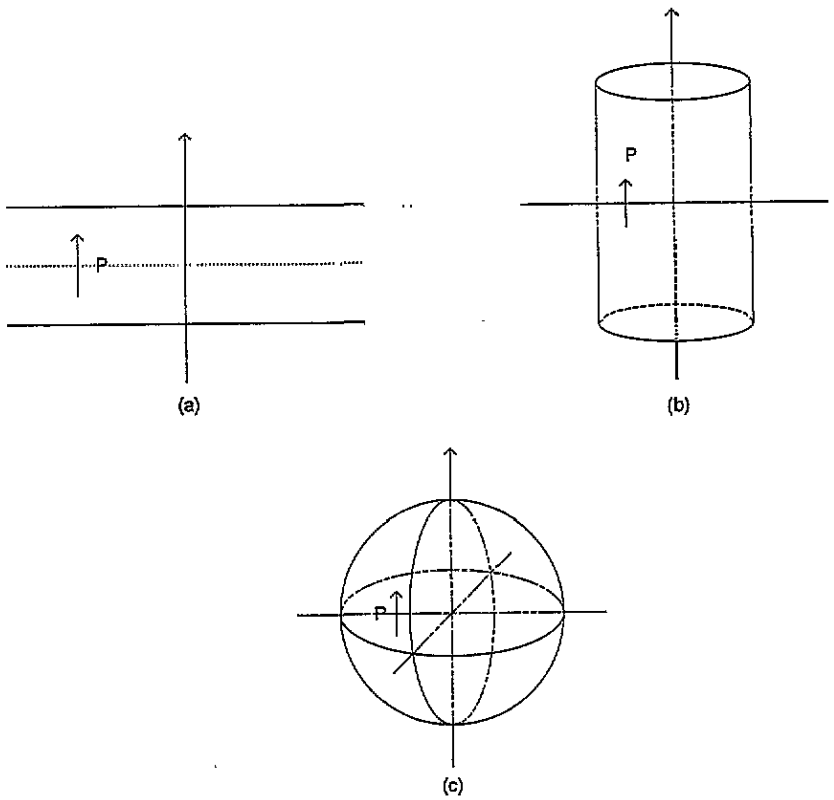

Figure 1. The geometries of ferroelectrics in the calculation.

In order to get the susceptibility profile $P(z)$ or $P(r)$ in the ferroelectric phase, we have to solve equations (2) and (5) simultaneously. First the differential equations are solved with suitable boundary conditions giving the profiles. At the same time, the free energy is obtained. If the free energy is negative, which means the ferroelectric phase is more stable than the paraelectric phase, the above calculation is accepted. When the free energy is positive, the polarization is reset to zero, and the susceptibility is recalculated. The mean susceptibility is obtained by integration of the susceptibility profile. This procedure is repeated for every size we have chosen.

In the paraelectric phase the solution of differential equation (5) under the boundary condition (6) gives the following expression for the susceptibility for the film geometry:

$$\chi(z) = -\chi_b + \chi_b \frac{\xi \cos(z/\xi)}{\xi \cos(d/2\xi) - \delta_f \sin(d/2\xi)} \tag{10}$$

where $\xi = \sqrt{-D/A}$, $\chi_b = -1/A$ is the bulk susceptibility and d the film thickness. For the cylinder geometry

$$\chi(r) = -\chi_b + \chi_b \frac{\xi J_0(r/\xi)}{\xi J_0(d/2\xi) - \delta_c J_1(d/2\xi)} \tag{11}$$

where J_0 and J_1 are zero-order and first-order Bessel functions and d is the diameter of the cylinder. For spheres

$$\chi(r) = -\chi_b + \chi_b \frac{d\xi \cos(r/\xi)}{2r[\delta_s \cos(d/2\xi) + (\xi - 2\delta_s)\sin(d/2\xi)]} \tag{12}$$

where d is its diameter. In the ferroelectric phase, equation (5) must be solved numerically.

The total susceptibility of a film is

$$\chi = \frac{1}{d}\int_{-d/2}^{d/2} \mathrm{d}z\ \chi(z) \tag{13}$$

and that for a cylinder is

$$\chi = \frac{8}{d^2}\int_0^{d/2} r\,\mathrm{d}r\ \chi(r) \tag{14}$$

and the average susceptibility of a sphere is

$$\chi = \frac{24}{d^3}\int_0^{d/2} r^2\,\mathrm{d}r\ \chi(r) \tag{15}$$

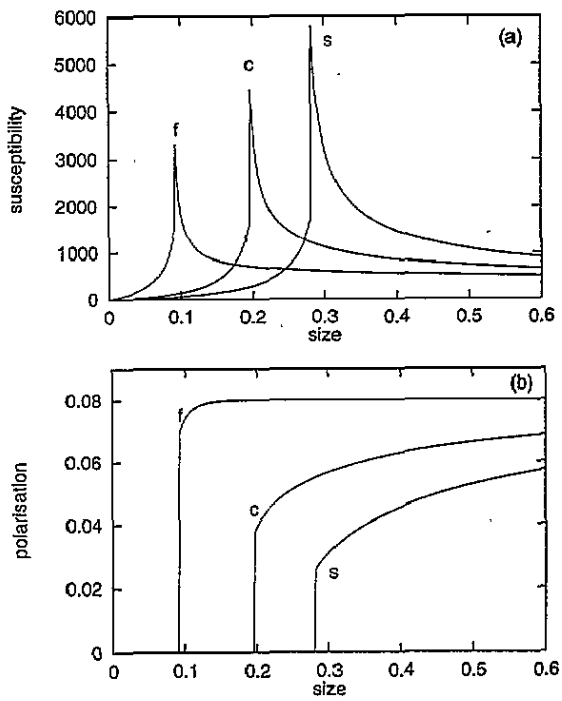

Figure 2. Size dependence of (a) relative susceptibility and (b) spontaneous polarization at the surface for $\delta_f = 43$ nm. The polarization is in units of C m^{-2}; the size is in units of μm. The meanings of symbols in the figure are: f—film geometry, c—cylinder geometry, s—sphere geometry.

The results presented in figures 2 and 3 are the size dependence of the susceptibility χ and the corresponding spontaneous polarization P for the free-standing film, cylinder and sphere. The model parameters adopted are appropriate to barium titanate, i.e. $A_0 = 6.66 \times 10^5$ J m C^{-2} K^{-1}, $B = -3.56 \times 10^9$ J m^{-5} C^{-4}, $C = 2.7 \times 10^{11}$ J m^9 C^{-6}, $D = 1.14 \times 10^{-7}$ J m^5 C^{-2}. The values of A_0, B and C are from the standard text [15] for

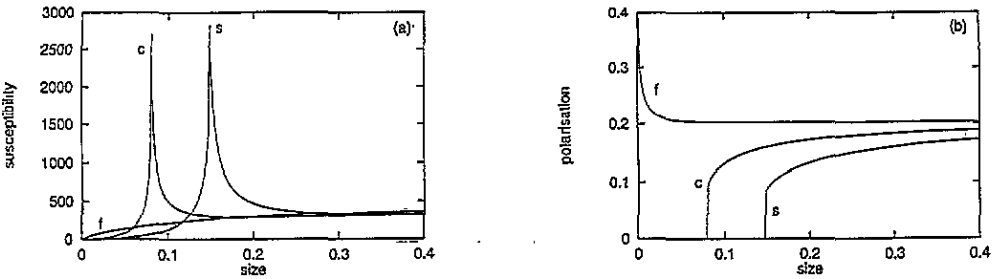

Figure 3. Size dependence of (a) relative susceptibility and (b) spontaneous polarization at the surface for $\delta_f = -43$ nm. The polarization is in units of C m^{-2}; the size is in units of μm. The meaning of symbols in the figure are: f—film geometry, c—cylinder geometry, s—sphere geometry.

bulk materials, and D and δ have been chosen tentatively to fit the Curie temperature of barium titanate particles [21, 22]. The temperature we used is $T = 70$ °C (the temperature of the measurements of [2]). Figure 2 is for $\delta_f = 43$ nm. It is obvious that there exists a size-driven phase transition of first order—the same order as the temperature-driven phase transition. The susceptibility is discontinuous but finite at the critical size, below which the polarization is zero. The critical size is about 100 nm for the film geometry, 200 nm for the cylinder geometry and around 300 nm for spheres. This type of variation with size occurs because in the sphere geometry the confinement involves all three dimensions, but only two dimensions are involved in the cylinder geometry, and a single dimension for the film. As the confinement dimensionality increases, the susceptibility maximum is enhanced around the critical size, whilst the polarization for a given size d is reduced.

The corresponding results for negative δ_f (enhanced surface ferroelectricity) are shown in figure 3. Compared to the results for positive δ_f, in the film case the polarization increases and the susceptibility decreases as the size decreases, and the size-driven phase transition vanishes, in agreement with results that have been obtained before [19, 18, 17, 20]. However, in the cylinder and sphere geometries, there still exits a size-driven phase transition and a corresponding critical size. This occurs because the extrapolation length δ is always positive at small enough size—recall equations (7)–(9). In other words, the ferroelectricity is always depressed at small size because of the decrease of the coordinate number. By comparing with figure 2 we can see that the critical size is shifted to smaller size, and the peak values at the critical size are reduced.

4. Comparison with experimental measurements

Experimental measurements that can be compared with our theoretical models have been carried out on ceramic or fine-grained films. Such samples can be considered as an assembly of ferroelectric spheres with a distribution of spherical particle size. As far as we are aware, there are as yet no suitable measurements corresponding to the single-crystal film and cylinder geometries. In order to compare our theory with the measurements, we therefore use only the sphere geometry, and assume a particle size distribution of a Gaussian form [12, 27], as described below. However the experimental measurements are not in better than qualitative agreement with each other at the present time. For example, the dielectric constant of barium titanate ceramic is reported to have a maximum at a size around 0.7 μm in [1], around 0.4 μm in [2] and no maximum is observed in [4]. For this reason, we do not attempt to make a direct quantitative comparison between our calculation and experimental

measurements.

We assume that the particle size d is distributed about an average size d_0 according to a Gaussian distribution function of the form

$$f(d) = f_0 \exp\left(-\frac{(d-d_0)^2}{2\sigma^2}\right) \tag{16}$$

where σ is the standard deviation and f_0 is the normalization factor. Application of this to the results of section 3 will produce curves renormalized by the size distribution. The results are shown in figures 4 and 5 for barium titanate and lead titanate respectively with standard deviation factor $\gamma = \sigma/d_0$ as 0.1 and 1.0. The parameters for barium titanate are the same as for the last section with the positive extrapolation length. The parameters for lead titanate are as follows [21, 22]: $A_0 = 2.79 \times 10^5$ J m C^{-2} K, $B = -1.62 \times 10^9$ J m^5 C^{-4}, $C = 4.23 \times 10^{11}$ J m^9 C^{-6}, $D = 4.5 \times 10^{-10}$ J m^5 C^{-2}, $\delta = 3$ nm; the temperature is taken as $T = 30$ °C.

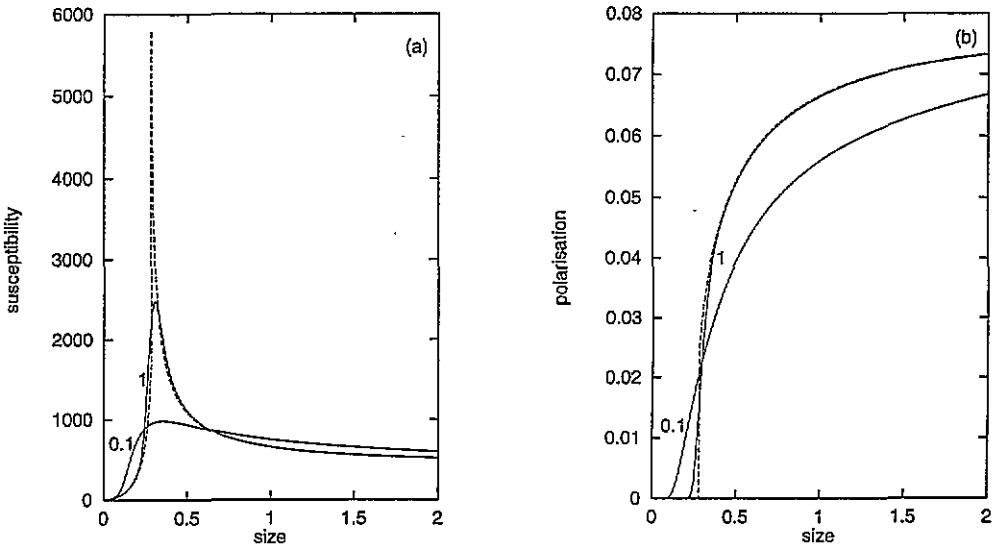

Figure 4. Average size dependence of (a) relative susceptibility and (b) polarization of barium titanate composite. The polarization is in units of C m^{-2}; the size is in units of μm. The dashed line is for isolated spheres. The standard deviation factor is given by the curve.

For samples with the smaller size distribution parameter γ, the only obvious effect of the renormalization occurs at around the critical size. The susceptibility peak is reduced and widened, but there is almost no change at sizes larger than about 30 nm in lead titanate and 1 μm in barium titanate. However, after the renormalization, the polarization smoothly decreases to zero at small size, making the phase transition appear quasi-second order, and there is also a slight decrease in the apparent critical size. The reason for this is as follows. Even if the average size of the particles corresponds to the paraelectric phase, as the result of the distribution of particle size there are still some particles of size large enough to be ferroelectric. Consequently the sample overall still exhibits weak ferroelectricity. This effect can be seen easily if we look at the curves with $\gamma = 1.0$. The apparent critical size is smaller size than that for $\gamma = 0.1$, and the polarization at large size is less than that of isolated particles of the corresponding size. The peak position in susceptibility shifts to smaller size, and the value of χ at large size is enhanced. This means that the anomaly

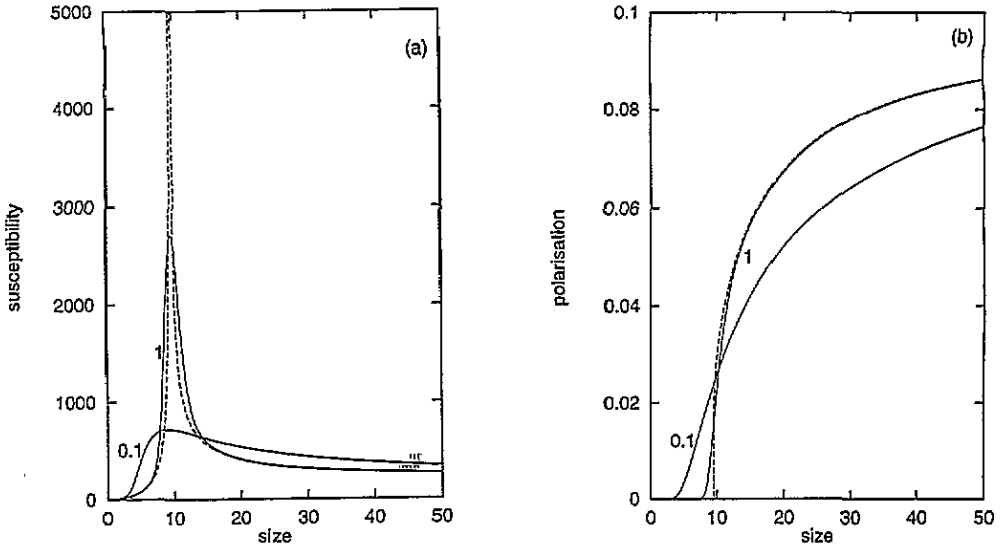

Figure 5. Average size dependence of (a) relative susceptibility and (b) polarization of lead titanate composite. The polarization is in units of C m^{-2}; the size is in units of nm.

in χ around the critical size can be substantially displaced from the single-particle critical size. However, the size-driven feature is still very obvious even though it is rather diffuse.

For barium titanate samples our theory predicts a peak value between 200 nm and 300 nm; experimental values range from below 100 nm [4, 5, 6] to 400 nm [2]. For lead titanate our theory gives a critical size of 10 nm; early dielectric constant measurements report 100 nm [3], but recent measurements show that the critical size is indeed about 10 nm [10, 11, 12].

5. Discussion and conclusions

Apart from the surface effect, temperature also plays an important role in the critical size. As the temperature increases, the critical size increases and the polarization is suppressed. In most of the experimental reports the temperature of the measurements is not explicitly mentioned, so we assume it to be room temperature. However, in some experiments, the sample may be heated up, so the temperature of the sample may be higher than that of the environment—room temperature. This could be another reason that for the same material, we have different critical sizes from different experimental measurements. For example, our calculation predicts that the critical size of an isolated sphere of barium titanate changes from 280 nm at 70 °C to 210 nm at 30 °C.

Generally there is always a size-driven phase transition in ferroelectrics with cylinder and sphere geometry. The size-driven phase transition is first order if its corresponding temperature-driven phase transition is first order. The susceptibility is much enhanced and the polarization is reduced at around the critical size. By comparing experimental measurements with our renormalized results for the sphere geometry, we find that our calculation is qualitatively in agreement with the dielectric measurements of barium titanate and lead titanate. The distribution of grain sizes makes the susceptibility and phase transition properties diffuse and shifts the critical size to smaller values.

References

[1] Arlt G, Hennings D and de With G 1985 *J. Appl. Phys.* **58** 1619
[2] Shaikh A S, Vest R W and Vest G M 1989 *IEEE Trans. Ultrason. Ferroelect. Freq. Control* **UFFC-36** 407
[3] Nakamura T, Takashige M, Terauchi H, Miura Y and Lawless W N 1984 *Japan. J. Appl. Phys.* **23** 1265
[4] Uchino K, Sadanaga E and Hirose T 1989 *J. Am. Ceram. Soc.* **72** 1555
[5] Yamamoto T, Urabe K and Banno H 1993 *Japan. J. Appl. Phys.* **32** 4272
[6] Schlag S and Eicke H F 1994 *Solid State Commun.* **94** 883
[7] Bachmann R and Bärner K 1988 *Solid State Commun.* **68** 865
[8] Freg M H and Payne D A 1993 *Appl. Phys. Lett.* **63** 2753
[9] Vest R W 1990 *Ferroelectrics* **102** 53
[10] Ishikawa K, Yoshikawa K and Okada N 1988 *Phys. Rev.* B **37** 5852
[11] Zhong W L, Jiang B, Zhang P L, Ma J M, Chen H M, Yang Z H and L Li X 1993 *J. Phys.: Condens. Matter* **5** 2619
[12] Ishikawa K, Okada N, Takada K, Nomura T and Hagina M 1994 *Japan. J. Appl. Phys.* **33** 3495
[13] Cho C R, Jang M S, Jeong S Y, Kim H J and Ro J H 1994 *Ferroelectrics* **152** 37
[14] Nagatomo T, Tanaka K, Yamanashi A and Omoto O 1994 *Ferroelectrics* **152** 133
[15] Mitsui T, Tatsuzaki I and Nakamura E 1976 *An Introduction to the Physics of Ferroelectrics* (New York: Gordon and Breach)
[16] Tilley D R and B Žekš 1984 *Solid State Commun.* **49** 823
[17] Qu B D, Jiang B, Wang Y G, Zhang P L and Zhong W L 1994 *Chinese Phys. Lett.* **11** 514
[18] Zhong W L, Wang Y G and Zhang P L 1994 *Phys. Lett.* **189A** 121
[19] Qu B D, Zhong W L, Wang K M and Wang Z L 1993 *Integrated Ferroelectr.* **3** 7
[20] Zhong W L, Qu D B, Zhang P L and Wang Y G 1994 *Phys. Rev.* B **50** 12375
[21] Wang Y G, Zhong W L and Zhang P L 1994 *Solid State Commun.* **90** 329
[22] Zhong W L, Wang Y G, Zhang P L and Qu D B 1994 *Phys. Rev.* B **50** 698
[23] Wang Y G, Zhang P L, Wang C L, Zhong W L, Napp N and Tilley D R 1995 *Chinese Phys. Lett.* **12** 110
[24] Blinc R and B Žekš 1974 *Soft Modes in Ferroelectrics and Antiferroelectrics* (Amsterdam: North-Holland)
[25] Lines M E and Glass A M 1977 *Principles and Applications of Ferroelectrics and Related Materials* (Oxford: Oxford University Press)
[26] Cottam M G, Tilley D R and Žekš B 1984 *J. Phys. C: Solid State Phys.* **17** 1793
[27] Jones F W 1938 *Proc. R. Soc.* A **166** 16